Available online at www.sciencedirect.com
SciVerse ScienceDirect
ELSEVIER
Ceramics International 39 (2013) 4099–4104
CERAMICS INTERNATIONAL
www.elsevier.com/locate/ceramint

Development of silver-containing diamond-like carbon for biomedical applications. Part I: Microstructure characteristics, mechanical properties and antibacterial mechanisms

Wen-Chien Lan[a,b], Shih-Fu Ou[c,d,e], Ming-Hong Lin[f], Keng-Liang Ou[a,c,d,**], Meng-Yuan Tsai[f,*]

[a]*Research Center for Biomedical Implants and Microsurgery Devices, Taipei Medical University, Taipei 110, Taiwan*
[b]*School of Dentistry, College of Oral Medicine, Taipei Medical University, Taipei 110, Taiwan*
[c]*Research Center for Biomedical Devices and Prototyping Production, Taipei Medical University, Taipei 110, Taiwan*
[d]*Graduate Institute of Biomedical Materials and Tissue Engineering, College of Oral Medicine, Taipei Medical University, Taipei 110, Taiwan*
[e]*Institute of Mold & Die Engineering, National Kaohsiung University of Applied Sciences, Kaohsiung, 807, Taiwan*
[f]*Department of Mechanical Engineering and Graduate Institute of Mechanical and Precision Engineering, National Kaohsiung University of Applied Sciences, Kaohsiung 807, Taiwan*

Received 4 September 2012; received in revised form 30 October 2012; accepted 30 October 2012
Available online 5 November 2012

Abstract

Nanosilver containing diamond-like carbon films with different silver fractions were synthesized by the radio frequency magnetron sputtering using a single silver target in an atmosphere of Ar/CH_4 mixture. The nanocrystalline silver clusters spontaneously segregated within an amorphous diamond-like carbon matrix. The amorphous-to-crystalline phase transformation resulted in both the surface hardness and electrical resistivity of the composite films decreasing with increasing the silver cluster size. The enlarged cluster size also increased the film surface roughness and water contact angle. All the films exhibited an anti-bacterium rate of over 93%, which evidenced that applying these composite films to anti-bacterium surface treatment is effective.

Keywords: B. Nanocomposite; Silver containing diamond-like carbon film; Sputtering; Anti-bacterium

1. Introduction

Amorphous hydrogenated carbon (a-C:H) films with various electrical, optical, chemical and mechanical properties can be synthesized by adjusting their compositions, hybridizations and microstructures [1,2]. They have been widely applied to protective, heat-conducting, hydrophobic, biocompatible and other functional surface treatments for decades [3–6]. Previous studies have indicated that the residual stress which the a-C:H films suffered raised with film thickness increased and it may result in film detachment [7–10]. To overcome this problem, doping metal elements or carbides in a-C:H films have been demonstrated as an effective method to reduce the residual stress [11–15]. Furthermore, adding metal elements in a-C:H films also improves the electric conductivity of films and enables new antimicrobial functions [15–17]. Some heavy metal elements, especially silver, has a long term and environment antimicrobial ability has a limited toxicity to mammalian cells have been reported [18]. The nanoscale silver and its compounds have been proven to be effective matters against multiple drug-resistant bacteria by hindering the respiration and division of bacteria. It is generally reported that metal ions may bind to thiol groups in enzymes and proteins, and be deposited on cell membranes or cell walls which inhibit cell division and disrupt membrane integration [19–21]. Therefore, silver containing carbon

*Corresponding author: Tel.: +886 7 3814526-5430; fax: +886 7 3835015.
**Co-Corresponding author.
E-mail address: mengyuan6826@gmail.com (M.-Y. Tsai), klou@tmu.edu.tw (Keng-Liang Ou).

0272-8842/$ - see front matter © 2012 Elsevier Ltd and Techna Group S.r.l. All rights reserved.
http://dx.doi.org/10.1016/j.ceramint.2012.10.264

coatings have been attempted via currently carbon deposition techniques [16,17,22,23]. For extending the selectivity of substrate materials and corresponding applications, these techniques nowadays utilize a plasma enhancement to lower down the process temperature [24–31]. Among these carbon deposition techniques, radio frequency (RF) magnetron sputtering is often employed because of its low cost, simplicity and wide use. The typical magnetron sputtering deposition of carbon usually utilizes a graphite target as RF plasma cathode and introduces additional hydrocarbon gas as a supplementary carbon source. In this study, the graphite target was substituted by a silver target, and the introduced methane gas became the main carbon source for deposits. The silver content in films was controlled by adjusting the RF power input on silver target. According to previous researches [16,17,22,23], due to the fact that silver is relatively inert with carbon, the silver content in films usually segregates from a-C:H matrix and results composite behaviors. The aim of this study is to investigate the correlations between silver content and physico-chemical properties of synthesized Ag/a-C:H films and to evaluate the applicability of these composite for antibacterial usages.

2. Materials and methods

2.1. Deposition of Ag/a-C:H composite films

The substrate material is glass with a size of 1 cm in diameter and 2 mm in thickness. After being cleaned in ultrasonic bath of acetone and ethanol then air dried, glass substrates were loaded into the deposition chamber. The distance between silver target and substrates was fixed at 60 mm. The silver target had a purity of 4 N and a diameter of 7.62 cm. The sputtering system and detail deposition procedures have been described in previous works [32,33]. After evacuating the chamber and heating the substrates to 200 °C, the methane–argon gas mixture in a same ratio of 1/1.5 was introduced and the RF plasma was triggered under a working pressure of 0.23 Pa. Five different target power input, 100 W, 150 W, 200 W, 250 W and 300 W, were applied respectively to synthesize films with different silver contents. A same film thickness of 1100 nm was controlled for films prepared in all conditions.

2.2. Characterizations of Ag/a-C:H composite films

The surface and cross-sectional morphologies of deposited films were observed by using a scanning electron microscope (SEM, JSM-6500) and an atomic force microscope (AFM, NanoMan NS4+D3100). The compositions of deposited films were analyzed by using the Energy dispersive X-ray spectrometer (EDX) attached on the scanning electron microscope. Due to the fact that hydrogen element is out of the detection limit of EDX, the actual silver fraction cannot be quantified. The ratio of measured Ag to C was used as an index for the silver content in films. A Raman spectrometer (BWTEK-MiniRam^{TM}II) was used to analyze the bonding of a-C:H matrix in films. The hardness of the deposited film was measured by nanoindentation (Asmec-UNAT-M) with a diamond indenter and a load of 3 mN. The electrical resistivity of films was calculated via multiplying sheet resistivity values from 4-point probe measurement by measured film thickness. The contact angles of deionized water drop on surfaces of film with different silver content were measured by image analyzing.

2.3. Antibacterial test

JIS Z2801:2000 was employed as a standard to test the antimicrobial efficacy of films. The bacterial strains used in this test were Gram-positive *Escherichia coli* (ATCC 8739). A single colony of the strain was first streaked from a frozen stock using the streak plate method on nutrition agar plates. Before bacterial inoculation, the suspension was diluted using a nutrition broth to a density of 4×10^5 CFU/ml and then dropped onto specimens for incubation at 37 °C and 95% humidity for a period of 24 h. Serial dilution of each corresponding specimen by the dilute buffer was performed to a concentration of 10^1, 10^2, 10^3, and 10^4 fold, respectively. 1 ml of each diluted inoculums was placed onto nutrition agar plate for further culture at 37 °C for 24 h. Number of grown bacterial colonies (C) were counted to obtain the number of bacteria adhering to the plate (N). The antibacterial activity calculated by Eq. (1) was recognized as the antibacterial effect.

$$\text{Antibacterial rate (AR)} = 100 \times \frac{(N_2 - N_1)}{N_2(\%)} \qquad (1)$$

N_1: number of bacteria adhering to the tested sample after 24 h incubation.
N_2: number of bacteria adhering to the blank glass substrate after 24 h incubation.

3. Results and discussion

The Ag/C ratio in films obtained at different target power conditions are shown in Fig. 1. The Ag/C ratio values of films deposited at target power of 100 W, 150 W, 200 W, 250 W and 300 W are 0.07, 0.20, 0.25, 1.05 and 2.50, respectively. The Ag/C ratio increases exponentially with target power. The samples of different Ag/C ratio are denoted by $Ag_{0.07}/C$, $Ag_{0.20}/C$, $Ag_{0.25}/C$, $Ag_{1.05}/C$ and $Ag_{2.50}/C$ in following figures and descriptions. The $Ag_{0.07}/C$ film exhibits an amorphous feature, but crystalline silver clusters appears in films with higher Ag/C ratio. Due to the low solubility and low activity of silver to carbon, the excess silver content segregates as secondary phase in carbon matrix. This kind of nanoclusters is commonly found in similar films which are doped by low solubility metal elements [15,22–24,34] The a-C:H matrixes

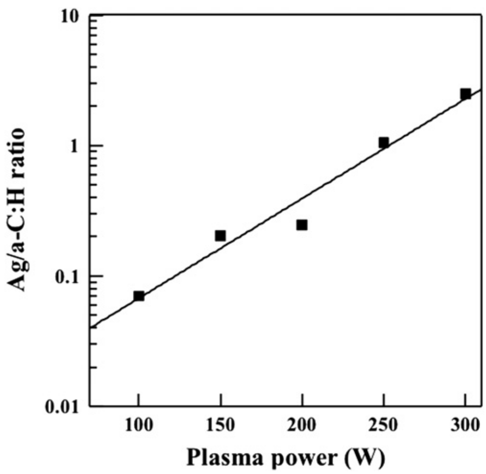

Fig. 1. Dependence of Ag/C ratio in film as a function of target power.

for all five different specimens remains an amorphous structure, but the fraction of sp^3 bond irregularly increases with the silver content. It has been reported that higher sp^3 bond fraction may increases the surface energy and affects the water contact angle and relative biocompatibility [35]. For the TEM images (Fig. 2), it is found that dark silver clusters distribute uniformly in brighter a-C:H matrix, but the size and the amount of silver clusters both increases with Ag/C ratio. Moreover, it is also found that the cluster size also increases gradually along the film growth direction. The selected area electron diffraction and convergent beam electron diffraction results demonstrated the clusters are the aggregations of silver nanocrystalline grains. This metal/a-C:H composite duplex phase structure should overall affect the electrical conductivity, mechanical performances and chemical properties of films.

The electrical resistivity of films in Fig. 3 and the surface hardness in Fig. 4 all confirms this. The highly conductive and relatively softer silver segregations indeed influence the electrical conductivity and mechanical performances of film. Both the resistivity and surface hardness of film decrease exponentially with the Ag/C ratio. The originally insulating a-C:H film can be altered into a conductive material by doping trace amount of silver. A conductive surface is advantageous for electrochemical applications or accelerating the ion releasing in antibacterial usages. However, comparing with the hardness of conventional a-C:H films, the hardness values of composite films tremendously decreases one order of magnitude. This is unfavorable for protective applications on tools.

In Fig. 2, it seems that the film surface is also rumpled along the cluster edge. The increase of cluster size might cause a higher surface roughness. The SEM and AFM 3D surface images shown in Fig. 5 evidence this, the surface roughness of films increases with the Ag/C ratio. The $Ag_{0.07}/C$ film is amorphous and displays a smooth film surface. When the Ag/C ratio reaches to 0.20, the silver clusters and granular features appear on films surface, and the measured root-mean-square average (RMS) roughness

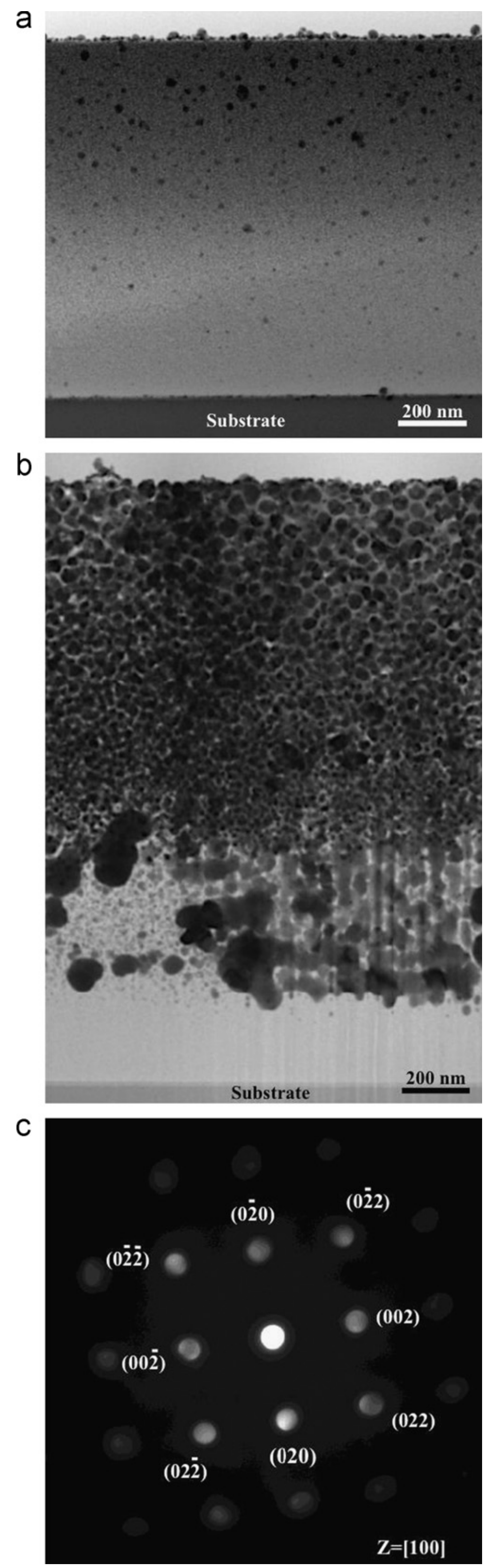

Fig. 2. TEM bright-field cross-sectional images of (a) $Ag_{0.07}/C$ and (b) $Ag_{2.50}/C$ films. The dark spheres with a diameter from 10 to 50 nm are Ag clusters. (c) The SADP of the cluster in Fig. 2(b).

value is increased but still is less than 5 nm. Once Ag/C ratio reached to 0.25, the surface roughness is suddenly raised to 9.4 nm. Such roughness change has a

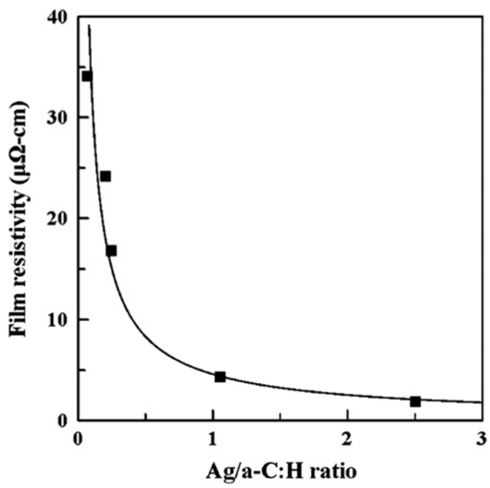

Fig. 3. Dependence of the film resistivity as a function of Ag/C ratio in films.

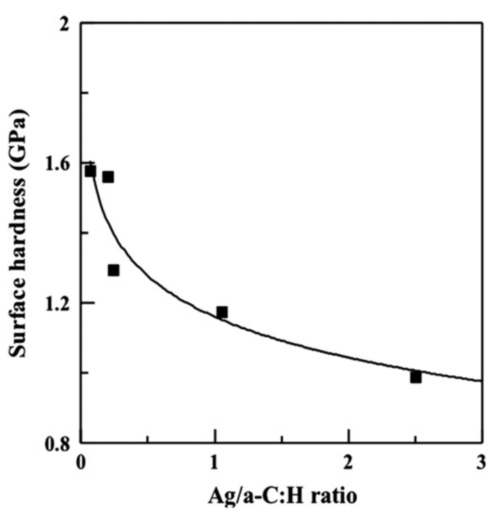

Fig. 4. Dependence of the film surface hardness as a function of Ag/C ratio in films and film thickness.

considerable influence on optical, tribological, wettability performances and consequent bacterial adhesion behavior on these Ag/a-C:H composite films. The water contact angle increases slightly with the surface roughness in nano-scale. A similar trend is also found in this work. The dependence of water contact angle on Ag/C ratio and surface roughness of film are shown in Fig. 6(a) and (b), respectively.

It seems that both the silver ratio and surface roughness enable the silver-incorporated a-C:H films to be more hydrophobic than conventional a-C:H films [35]. However, because the differences in surface roughness are small, it might only somewhat influence the water contact angle. Such large surface energy change is mainly resulted from the presence of silver clusters. A hydrophobic surface can be used as anti-sticking and antimicrobial applications.

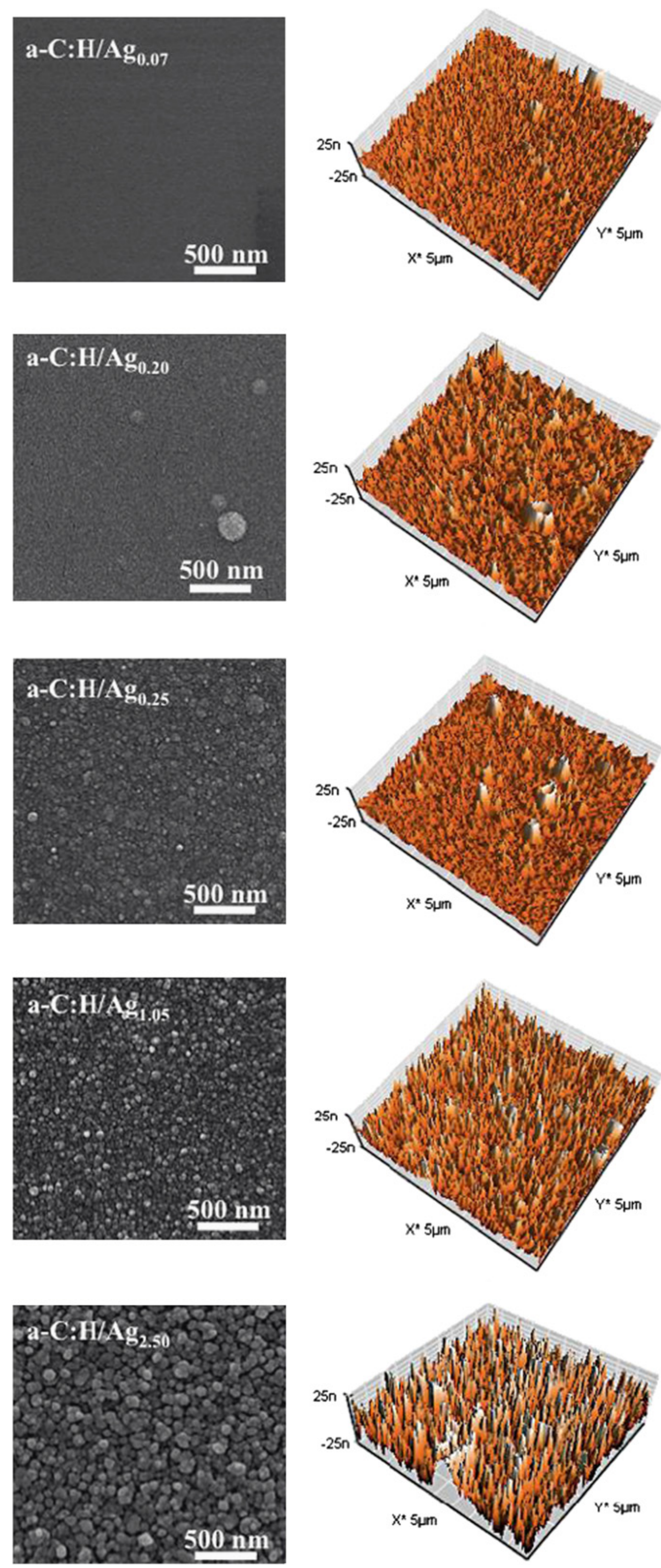

Fig. 5. SEM and AFM 3D surface images of films with different Ag/C ratio.

It has been proven that silver content in similar films can inhibit the adhesion of bacteria on film surface [36,37].

The antibacterial test results are shown in Table 1. Although the $Ag_{0.07}/C$ film has the lowest Ag content and shows the lowest antimicrobial performance in this study, its efficacy still reaches to 93%, even then this film does not exhibit observable silver nanoclusters structure and improve the wettability. All other Ag/a-C:H films in this study exhibit an excellent over 96% antimicrobial rates. The maximum antibacterial rates of 98% are found on the films with an over 0.25 Ag/C ratio, and no statistical difference between them. In our previous work [38], it has been proven that the Ag precipitates in a composite structure can release Ag^{+} ions to kill bacteria by destroying cell walls and cell membranes of *Escherichia coli* which results in the leakage of cytoplasm. These results again demonstrate the effectiveness of such antimicrobial silver–carbon composite films.

On the whole, adding silver does enhance the electrical conductivity, hydrophobic and antimicrobial performances of a-C:H films, but is accompanied with the drawback of lower hardness. Excess silver content does not further improve the antimicrobial efficacy, but causes decrease of surface hardness and flatness.

4. Conclusions

This study fabricated composite films comprising silver nanoclusters in hydrogenated carbon matrix on glass by the reactive radio frequency magnetron sputtering using a single silver target in an atmosphere of Ar/CH_4 mixture. The films with different silver content were deposited by adjusting the power inputs of silver target. The silver in films spontaneously segregated as nanocrystalline clusters dispersing in the a-C:H matrix. The size of cluster increased with the silver content, which results in the decreases in the surface hardness and electrical resistivity of the composite films. The increase of cluster size also raised the surface roughness and improved the wettability of the films. In addition, all the composite films exhibited anti-bacterium rate of over 93%, which evidenced the applicability of applying such composite film for anti-bacterium surface treatment.

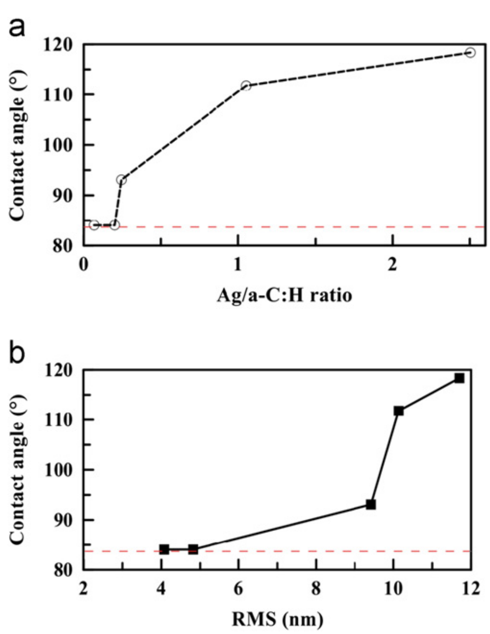

Fig. 6. (a) Dependence of the water contact angle as functions of Ag/C ratio in films. (b) Dependence of the water contact angle as functions of film surface roughness. The dash line is the water contact angle on conventional PECVD a-C:H film.

References

[1] P.K. Bachmann, R. Messier, Emerging technology of diamond thin films, Chemical and Engineering News 67 (1989) 24–39.
[2] K.E. Spear, Growth of crystalline diamond from low pressure gases, Earth and Mineral Science 56 (1987) 53–59.
[3] K. Jia, Y.Q. Li, T.E. Fischer, B. Gallois, Tribology of diamond-like carbon sliding against itself, silicon nitride, Journal of Materials Research 10 (1995) 1403–1410.
[4] C. Jaoul, O. Jarry, P. Tristant, T. Merle-Mejean, M. Colas, C. Dublanche-Tixier, J.M. Jacquet, Raman analysis of DLC coated engine components with complex shape: understanding wear mechanisms, Thin Solid Films 518 (2009) 1475–1479.
[5] A. Grill, Diamond-like carbon coatings as biocompatible materials—an overview, Diamond and Related Materials 12 (2003) 166–170.
[6] G. Dearnaley, J.H. Arps, Biomedical applications of diamond-like carbon (DLC) coatings: a review, Surface and Coatings Technology 200 (2005) 2518–2524.
[7] V.N. Inkin, G.G. Kirpilenko, A.J. Kolpakov, Internal stresses in ta-C films deposited by pulse arc discharge method, Diamond and Related Materials 10 (2001) 1103–1108.
[8] N. Mutsukuza, S. Tomita, Y. Mizum, The mechanical properties of hydrogenated hard carbon films, Thin Solid Film 214 (1992) 58–62.
[9] Akira Doi, Hiromu Kawai, Takashi Yoshioka, Shosaku Yamanaka, Vapor-deposited ceramic coating: status and prospects, Ceramic International 18 (1992) 223–229.
[10] A. Grill, Review of the tribology of diamond-like carbon, Wear 168 (1993) 143–153.
[11] A. Grill, V. Patel, Tribological properties of diamond-like carbon and related materials, Diamond and Related Materials 2 (1993) 597–605.
[12] K.A. Pischow, J. Koskinen, M. Adamik, P.B. Barna, Cross-sectional scanning force microscopy analysis of arc-discharge-deposited diamond-like carbon films, Ceramic International 22 (1996) 49–52.
[13] A.M. Peters, M. Nastasi, Titanium-doped hydrogenated DLC coatings deposited by a novel OMCVD-PIIP technique, Surface and Coatings Technology 167 (2003) 11–15.
[14] A.A. Voevodin, J.M. Schneider, C. Caperaa, P. Stevenson, A. Matthews, Characterisation of a saddle field source for deposition of diamond-like carbon films, Ceramic International 22 (1996) 1–5.

Table 1
Antibacterial rates of investigated samples.

	Blank glass	$a\text{-}C{:}H/Ag_{0.07}$	$a\text{-}C{:}H/Ag_{0.20}$	$a\text{-}C{:}H/Ag_{0.25}$	$a\text{-}C{:}H/Ag_{1.05}$	$a\text{-}C{:}H/Ag_{2.50}$
Antibacterial rate (%)	0	93 ± 2.2	96 ± 1.7	98 ± 1.2	96 ± 2.7	96 ± 1.6

[15] Y.H. Chan, C.F. Huang, K.L. Ou, P.W. Peng, Mechanical properties and antibacterial activity of copper doped diamond-like carbon films, Surface and Coatings Technology 206 (2011) 1037–1040.

[16] S.C.H. Kwok, W. Zhang, G.J. Wan, D.R. McKenzie, M.M.M. Bilek, Paul K. Chu, Hemocompatibility and anti-bacterial properties of silver doped diamond-like carbon prepared by pulsed filtered cathodic vacuum arc deposition, Diamond and Related Materials 16 (2007) 1353–1360.

[17] O. Garcia-Zarco, S.E. Rodil, M.A. Camacho-López, Deposition of amorphous carbon–silver composites, Thin Solid Films 518 (2009) 1493–1497.

[18] T.N. Kim, Q.L. Feng, J.O. Kim, J. Wu, H. Wang, G.C. Chen, F.Z. Cui, Antimicrobial effects of metal ions (Ag(+), Cu(2+), Zn(2+)) in hydroxyapatite, Journal of Materials Science: Materials in Medicine 9 (1998) 129–134.

[19] A.D. Russell, W.B. Hugo, 7 Antimicrobial activity and action of silver, Progress in Medicinal Chemistry 31 (1994) 351–358.

[20] V. Alt, T. Bechert, P. Steinrücke, M. Wagener, P. Seidel, E. Dingeldein, E. Domann, R. Schnettler, An in vitro assessment of the antibacterial properties and cytotoxicity of nanoparticulate silver bone cement, Biomaterials 25 (2004) 4383–4391.

[21] X.B. Tian, Z.M. Wang, S.Q. Yang, Z.J. Luo, Ricky K.Y. Fu, Paul K. Chu, Antibacterial copper-containing titanium nitride films produced by dual magnetron sputtering, Surface and Coatings Technology 201 (2007) 8606–8609.

[22] H.W. Choi, J.H. Choi, K.R. Lee, J.P. Ahn, K.H. Oh, Structure and mechanical properties of Ag-incorporated DLC films prepared by a hybrid ion beam deposition system, Thin Solid Films 516 (2007) 248–251.

[23] K. Baba, R. Hatada, S. Flege, W. Ensinger, Preparation and properties of Ag-containing diamond-like carbon films by magnetron plasma source ion implantation, Advances in Materials Science and Engineering (2012) Article ID 536853(5pp.), http://dx.doi.org/10.1155/2012/536853.

[24] C. Nørgård, S.S. Eskildsen, A. Matthews, Engineering applications for diamond-like carbon, Surface and Coatings Technology 74–75 (1995) 358–361.

[25] S.J. Dowey, K.M. Read, K.S. Fancey, A. Matthews, The penetration into blind holes of diamond-like carbon films produced by rf plasma assisted CVD, Surface and Coatings Technology 74–75 (1995) 710–716.

[26] X.M. He, W.Z. Li, H.D. Li, Ion beam assisted deposition of diamond-like carbon onto steel materials: preparation and advantages, Surface and Coatings Technology 84 (1996) 414–419.

[27] J. Deng, M. Braun, DLC multiplayer coatings for wear protection, Diamond and Related Materials 4 (1995) 936–943.

[28] N.A. Sánchez, C. Rincón, G. Zambrano, H. Galindo, P. Prieto, Characterization of diamond-like carbon (DLC) thin films prepared by r.f. magnetron sputtering, Thin Solid Films 373 (2000) 247–250.

[29] D.Y. Wang, K.W. Weng, C.L. Chang, X.J. Guo, Tribological performance of metal doped diamond-like carbon films deposited by cathodic arc evaporation, Diamond and Related Materials 9 (2000) 831–837.

[30] V.N. Inkin, G.G. Kirpilenko, A.A. Dementjev, K.I. Maslakov, A superhard diamond-like carbon film, Diamond and Related Materials 9 (2000) 715–721.

[31] R.F. Huang, C.Y. Chan, C.H. Lee, K.Y. Li, L.S. Wen, C. Sun, Wear-resistant multilayered diamond-like carbon coating prepared by pulse biased arc ion plating, Diamond and Related Materials 10 (2001) 1850–1854.

[32] H.C. Cheng, S.Y. Chiou, C.M. Liu, M.H. Lin, C.C. Chen, K.L. Ou, Effect of plasma energy on enhancing biocompatibility and hemocompatibility of diamond-like carbon film with various titanium concentrations, Journal of Alloys and Compounds 477 (2009) 931–935.

[33] W.C. Feng, C.H. Wang, H.C. Cheng, S.Y. Chiou, C.S. Chen, K.L. Ou, Enhancement of hemocompatibility on titanium implant with titanium-doped diamond-like carbon film evaluated by cellular reactions using bone marrow cell cultures in vitro, Journal of Vacuum Science and Technology B 27 (2009) 1559–1565.

[34] R. Paul, S. Dalui, A.K. Pal, Modulation of field emission properties of DLC films with the incorporation of nanocrystalline silver nanoparticles by CVD technique, Surface and Coatings Technology 204 (2010) 4025–4033.

[35] H.W. Choi, R.H. Dauskardt, S.C. Lee, K.R. Lee, K.H. Oh, Characteristic of silver doped DLC films on surface properties and protein adsorption, Diamond and Related Materials 17 (2008) 252–257.

[36] A. Okada, T. Nikaido, M. Ikeda, K. Okada, J. Yamauchi, R.M. Foxton, H. Sawada, J. Tagami, K. Matin, Inhibition of biofilm formation using newly developed coating materials with self-cleaning properties, Dental Materials Journal 27 (2008) 565–572.

[37] C. Price, M.G.J. Waters, D.W. Williams, M.A.O. Lewis, D. Stickler, Surface modification of an experimental silicone rubber aimed at reducing initial candidal adhesion, Journal of Biomedical Materials Research 63 (2002) 122–128.

[38] C.F. Huang, H.J. Chiang, W.C. Lan, H.H. Chou, K.L. Ou, C.H. Yu, Development of silver-containing austenite antibacterial stainless steels for biomedical applications Part I: microstructure characteristics, mechanical properties and antibacterial mechanisms, Biofouling 27 (2011) 449–457.